

THE UV-BRIGHT QUASAR SURVEY (UVQS): DR1

TALAWANDA R. MONROE¹, J. XAVIER PROCHASKA², N. TEJOS², G. WORSECK³, JOSEPH F. HENNAWI³, TOBIAS SCHMIDT³,
JASON TUMLINSON¹, YUE SHEN⁴

Draft version October 13, 2018

ABSTRACT

We present the first data release (DR1) from our UV-bright Quasar Survey (UVQS) for new $z \sim 1$ active galactic nuclei (AGN) across the sky. Using simple GALEX UV and WISE near-IR color selection criteria, we generated a list of 1450 primary candidates with $FUV < 18.5$ mag. We obtained discovery spectra, primarily on 3m-class telescopes, for 1040 of these candidates and confirmed 86% as AGN with redshifts generally at $z > 0.5$. Including a small set of observed secondary candidates, we report the discovery of 217 AGN with $FUV < 18$ mag that had no previously reported spectroscopic redshift. These are excellent potential targets for UV spectroscopy before the end of the *Hubble Space Telescope* mission. The main data products are publicly released through the Mikulski Archive for Space Telescopes.

Subject headings: intergalactic medium – quasars

1. INTRODUCTION

Presently, the only efficient means of studying the diffuse gas surrounding galaxies (a.k.a. halo gas or the circumgalactic medium, CGM) and in between galaxies (a.k.a. the intergalactic medium, IGM) is through absorption-line spectroscopy of luminous, background quasars (e.g. Tripp et al. 2008; Tumlinson et al. 2013; Tejos et al. 2014). Furthermore, because the principal transitions to diagnose gas lie at far-ultraviolet (FUV) wavelengths ($\lambda_{\text{rest}} < 2000\text{\AA}$), for $z < 1$ studies one requires UV spectrometers on space-borne facilities. Currently, and for the foreseeable future, the Hubble Space Telescope (*HST*) affords the only opportunity for such research, primarily with the Cosmic Origins Spectrograph (COS). Given the modest aperture of *HST*, these observations are generally restricted to the brightest FUV quasars on the sky.

High-quality, FUV spectroscopy of $z \sim 1$ quasars have enabled several, unique experiments to study the CGM and IGM of the universe over the past ~ 10 Gyr. These include: (1) the survey of highly ionized gas via the NeVIII $\lambda\lambda 770, 780$ doublet and/or broad H I Ly α systems that may trace the elusive warm-hot ionized medium (WHIM; e.g. Lehner et al. 2007; Meiring et al. 2013; Tejos et al. 2015); (2) the search for signatures of galactic and AGN feedback (e.g. Tripp et al. 2011); (3) the measurements of enrichment in galactic halos and optically thick gas (e.g. Lehner et al. 2013; Werk et al. 2013, 2014); and (4) revealing the structure of the cosmic web and its correlation to the large-scale structures traced by galaxies (e.g. Tejos et al. 2014). While each of these programs has had scientific impact, they are limited by

sample variance.

An efficient way to increase the volumes surveyed is to focus on those bright UV QSOs that maximize the redshift path covered, i.e. those with $z_{\text{em}} \gtrsim 1$. To date, only a small number of $z \sim 1$ quasars have been observed with *HST*, primarily corresponding to the set of sources with very high FUV flux. These have been drawn from historical, large-area surveys for AGN (e.g. the Palomar-Green Bright Quasar Survey and the Hamburg/ESO survey) and more recently the Northern Galactic pole footprint of the Sloan Digital Sky Survey (SDSS). Cross-matching the quasar sample of Flesch (2015) against the point-source catalog of the GALEX survey, one recovers ≈ 140 sources with $z > 0.6$ and $FUV < 18$ mag (fewer than 50 at $z > 1$). These are preferentially located within the SDSS footprint which has extensively surveyed the Northern galactic pole for quasars (e.g. Schneider et al. 2010). Given that *HST* may observe nearly any position on the sky, we are motivated to perform an all-sky search for new, FUV-bright quasars across the sky. Indeed, progress in this area demands the discovery of new FUV-bright quasars.

The principal goal of our survey is to provide the community with a nearly complete set of UV-bright, AGN before the termination of the *HST* mission. We recognized that the combination of two NASA imaging missions – GALEX and WISE – enables a modern, all-sky search for UV bright quasars. These must be spectroscopically confirmed, however, before subsequent *HST* observations. Given our interest in FUV-bright sources, this implies optically bright candidates that can be spectroscopically confirmed on 3m-class telescopes. The following manuscript provides the first data release (DR1) from our UV-bright Quasar Survey (UVQS). The main data products are available at the Mikulski Archive for Space Telescopes⁵.

This paper is organized as follows. Section 2 describes the UVQS candidate selection, focused on detecting $z \sim 1$ quasars with $FUV < 18$ mag. The follow-up

¹Space Telescope Science Institute, Baltimore, MD, 21218, USA

²Department of Astronomy and Astrophysics, UCO/Lick Observatory, University of California, 1156 High Street, Santa Cruz, CA 95064, USA

³Max-Planck-Institut für Astronomie, Königstuhl 17, D-69115 Heidelberg, Germany

⁴Department of Astronomy and National Center for Supercomputing Applications, University of Illinois at Urbana-Champaign, Urbana, IL 61801, USA

⁵ <https://archive.stsci.edu/prepds/uvqs>

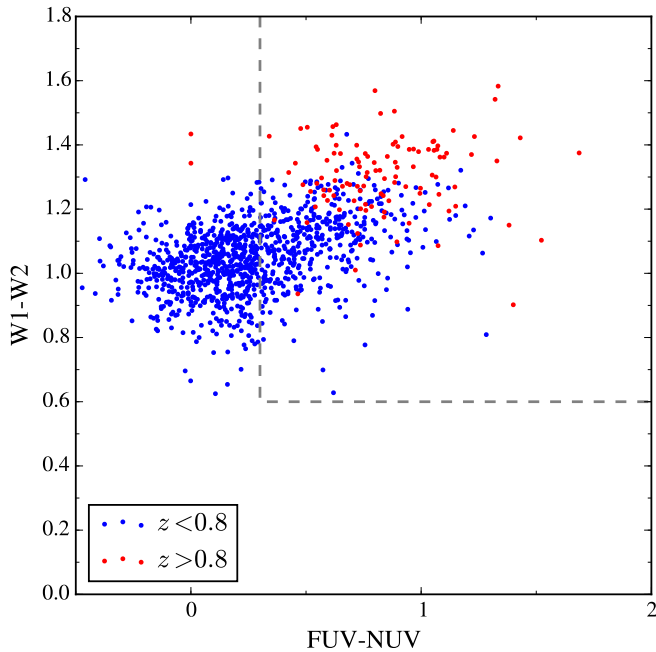


FIG. 1.— Color-color plot of WISE and GALEX photometry of the SDSS DR7 quasars (Schneider et al. 2010) that have a NUV flux < 19 mag. It is evident that each has a $W1 - W2 > 0.6$ mag color, consistent with the Stern et al. (2012) selection-criteria for AGN. Furthermore, the $z > 0.8$ quasars exhibit redder $FUV - NUV$ colors which we hypothesize results from intervening Lyman limit opacity. The gray dashed lines at $W1 - W2 = 0.6$ mag and $FUV - NUV = 0.3$ mag indicate the color-color criteria adopted for our primary candidates (Table 1).

spectroscopy is discussed in Section 3 and the redshift analysis is described in Section 4. We present the primary results in Section 5. When relevant, we assume a Λ CDM cosmology with $h = 0.7$, $\Omega_m = 0.3$, and $\Omega_\Lambda = 0.7$.

2. THE UVQS CANDIDATES

With the explicit goal of discovering new FUV-bright quasars at $z \sim 1$ across the sky, we developed color-color criteria leveraging the all-sky surveys of the WISE and GALEX missions to: (i) isolate AGN; and (ii) maximize the probability that these AGN lay at $z_{\text{em}} \gtrsim 1$. For the first criterion, we followed the impressive results from the WISE team who demonstrated the clean separation of AGN from stars, galaxies and other astrophysical sources using WISE photometry (Stern et al. 2012). Specifically, Stern et al. (2012) showed that AGN tend to exhibit $W1 - W2 > 0.4$ mag with galaxies and stars having smaller values. Although this criterion may not capture all AGN (e.g. Assef et al. 2010), we strongly expect that every UV-bright AGN satisfies the criterion. Indeed, we find that of the 1148 quasars at $z < 1.5$ from SDSS DR7 detected by GALEX ($NUV < 19.0$), all have $W1 - W2 > 0.625$ mag (Figure 1). The overwhelming majority of these have $z < 0.8$ (90%).

Figure 1 also shows the $FUV - NUV$ colors of these quasars. These were measured from the “photoobjall” catalog of the GALEXGR6Plus7 context at MAST and improved, where possible, using the MIS catalog (“bcscat_mis” Bianchi et al. 2014). We see that the majority of $z < 0.8$ quasars have $FUV - NUV < 0.3$ mag (60%) and that nearly all of the $z > 0.8$ quasars have a redder $FUV - NUV$ color. We believe that this ‘reddening’ pri-

marily results from the presence of one or more Lyman limit systems (LLSs) in the redshift interval $0.5 < z < 0.8$ whose continuum opacity reduces only the FUV flux. We infer that nearly every $z \sim 1$ quasar exhibits at least one intervening LLS⁶ with $N_{\text{HI}} > 10^{16.7} \text{ cm}^{-2}$.

With our photometric criteria established,

$$W1 - W2 > 0.6 \text{ mag} \quad (1)$$

$$FUV - NUV > 0.3 \text{ mag} \quad (2)$$

$$FUV < 18.5 \text{ mag}, \quad (3)$$

we cross-matched every source in the GALEXGR6Plus7 catalogs⁷ satisfying these criteria against the AllWISE Source Catalog. To avoid selecting already known quasars given the beam sizes of WISE and GALEX, we then eliminated any sources that lay within $5''$ of a UV-bright quasar from SDSS DR7. This generated a list of 1450 primary candidates (Table 1). We discovered, during our analysis, that this candidate list includes hundreds of previously cataloged sources from other surveys. This includes the SDSS-III survey which included WISE-selected quasar targets (Paris et al. 2015). Their primary WISE criteria, however, precluded overlap with our sample. Given that several of these surveys have known examples of false redshift identifications or do not provide the discovery spectra, we maintained the list and re-observed many of the brighter sources ($FUV < 18$ mag). Figure 2 shows an all-sky summary of the UVQS candidates, separated by FUV flux. The exclusion of the Galactic plane is obvious and the lower incidence of sources in the SDSS footprint is notable.

In several of the observing runs, conditions were unexpectedly favorable and we exhausted the primary candidates at certain RA ranges. To fill the remaining observing time, we generated a secondary candidate list with one criterion modified: $-0.5 < FUV - NUV < 0.3$. This would permit a much higher fraction of low- z AGN, but may also yield a few sources at $z \sim 1$. This secondary set of candidates is provided in Table 2.

3. OBSERVATIONS AND DATA PROCESSING

We proceeded to obtain discovery-quality longslit spectra (i.e. low-dispersion, large wavelength coverage, modest signal-to-noise (S/N) of our UVQS candidates in one calendar year. Our principal facilities were: (i) the dual Kast spectrometer on the 3m Shane telescope at Lick Observatory; (ii) the Boller & Chivens (BCS) spectrometer on the Irénée du Pont 100” telescope at Las Campanas Observatory; and (iii) the Calar Alto Faint Object Spectrograph (CAFOS) on the CAHA 2.2m telescope at Calar Alto Observatory (CAHA). We acquired an additional ≈ 20 spectra on larger aperture telescopes (Keck/ESI, MMT/MBC, Magellan/MagE) during twilight or under

⁶ In standard IGM nomenclature, LLS with $N_{\text{HI}} < 10^{17.3} \text{ cm}^{-2}$ are often referred to as partial LLS or pLLS.

⁷ Our explicit cassjobs query for the AIS data was: select objid, ra, dec, fuv_mag as fuv, nuv_mag as nuv from photoobjall; where fuv_mag BETWEEN 12. and 18.5; and (fuv_mag-nuv_mag) BETWEEN -0.5 and 2.0; and fuv_mag > -999; and nuv_mag > -999. We then used the following for the MIS to improve the photometry: select objid, ra, dec, fuv_mag as fuv, nuv_mag as nuv from bcscat_mis; where fuv_mag BETWEEN 12. and 18.5; and (fuv_mag-nuv_mag) BETWEEN -0.5 and 2.0; and fuv_mag > -999; and nuv_mag > -999.

TABLE 1
UVQS DR1 PRIMARY CANDIDATES

Name	α_{J2000} (deg)	δ_{J2000} (deg)	W1 (mag)	W2 (mag)	FUV (mag)	NUV (mag)
UVQSJ000000.15–200427.7	0.00064	–20.07437	13.55	12.54	18.27	17.97
UVQSJ000002.92–350332.6	0.01218	–35.05905	12.69	11.55	17.61	17.31
UVQSJ000009.66–163441.5	0.04023	–16.57819	13.43	12.19	18.48	17.72
UVQSJ000037.52–752442.6	0.15633	–75.41184	11.69	10.63	17.81	17.45
UVQSJ000355.89–224122.4	0.98286	–22.68955	13.24	12.11	17.97	17.24
UVQSJ000503.70–391747.9	1.26542	–39.29664	12.26	11.12	17.82	17.23
UVQSJ000609.57–261140.6	1.53989	–26.19460	13.31	12.12	18.16	17.53
UVQSJ000613.29+321534.6	1.55537	32.25960	12.93	11.75	18.42	17.95
UVQSJ000717.70+421646.7	1.82374	42.27963	12.44	11.51	18.09	17.61
UVQSJ000741.01–635145.9	1.92085	–63.86274	12.65	11.45	17.96	17.41
UVQSJ000750.79+031733.1	1.96161	3.29253	12.98	11.58	17.80	17.01
UVQSJ000755.68+052818.8	1.98200	5.47189	13.12	11.73	18.07	17.29
UVQSJ001444.03–223522.6	3.68344	–22.58961	13.16	11.77	18.39	17.34

NOTE. — Table 1 is published in its entirety in the electronic edition, a portion is shown here for guidance regarding its form and content.

TABLE 2
UVQS DR1 SECONDARY CANDIDATES

Name	α_{J2000} (deg)	δ_{J2000} (deg)	W1 (mag)	W2 (mag)	FUV (mag)	NUV (mag)
UVQSJ000007.85–633535.2	0.03271	–63.59311	13.25	12.32	18.06	17.77
UVQSJ000011.73+052317.4	0.04886	5.38818	11.90	10.88	18.37	18.30
UVQSJ000024.03–275153.5	0.10013	–27.86486	12.85	11.80	18.32	18.14
UVQSJ000024.42–124547.9	0.10173	–12.76331	11.08	10.08	15.82	15.78
UVQSJ000036.68–634123.7	0.15285	–63.68991	12.44	11.46	18.10	18.15
UVQSJ000053.51–443933.5	0.22297	–44.65930	12.56	11.81	17.95	17.95
UVQSJ000054.29+183021.4	0.22621	18.50594	13.26	12.18	16.65	16.47
UVQSJ000055.97+172338.9	0.23320	17.39414	13.13	12.09	17.71	17.83
UVQSJ000103.53–114725.9	0.26469	–11.79053	12.70	11.59	18.04	18.13
UVQSJ000115.89+051902.1	0.31621	5.31725	13.47	12.61	18.43	18.44
UVQSJ000118.99+172425.3	0.32913	17.40703	12.86	11.88	18.48	18.33
UVQSJ000128.58–320842.1	0.36908	–32.14502	13.17	12.05	18.30	18.03
UVQSJ000146.09–765714.3	0.44203	–76.95396	11.01	10.23	17.05	16.88
UVQSJ000150.56+111647.3	0.46068	11.27981	11.68	10.73	17.27	17.12
UVQSJ000200.53–073907.5	0.50220	–7.65209	14.11	13.01	18.19	18.13
UVQSJ000210.06+171558.2	0.54193	17.26616	15.50	14.85	18.46	18.16

NOTE. — Table 2 is published in its entirety in the electronic edition, a portion is shown here for guidance regarding its form and content.

poor observing conditions. Typical exposure times were limited to $\lesssim 200$ s with adjustments for fainter sources or sub-optimal observing conditions. Table 3 provides a list of the observed candidates.

The two-dimensional (2D) spectral images and calibration frames were reduced with custom software, primarily the LowRedux package⁸ developed by J. Hennawi, X. Prochaska, and D. Schlegel. Briefly, the images were bias subtracted, flat-fielded using quartz lamp spectral images, and wavelength calibrated with arc lamp exposures. Objects within the slit were automatically identified and optimally extracted to generate 1D spectra. These were fluxed after generating a sensitivity function from observations of spectrophotometric standard stars taken during each observing run. We did not carefully account for varying atmospheric conditions nor did we correct for slit-losses from variable seeing or atmospheric dispersion. Therefore, the reported fluxes are crude and not even especially accurate in a relative sense, partic-

ularly at the wavelength extrema. Although we occasionally obtained multiple exposures for a given source, these were not combined; the highest quality spectrum was analyzed. Upon visual inspection we assigned a spectral data quality number (SPEC_QUAL) to each spectrum. Our scale spans 0 to 5, in which 0 is poor, or unusable, and 5 is excellent. SPEC_QUAL values are a good proxy for S/N ratio and are included in Table 3. Note, even spectra without spectral features may have a high SPEC_QUAL value.

The calibrated 1D spectra are published in DR1 and provided at <https://archive.stsci.edu/prepds/uvqs>. We also present a cutout, optical image of each source taken from the SDSS or DSS survey. Figure 3 shows representative spectra from the UVQ DR1 sample, including examples of a Galactic star, a low- z AGN, and a $z > 1$ quasar (PHL 1288). At the S/N of these spectra (each of which has a spectral quality of 4 or 5), redshift identification is straightforward. We note that $\approx 50\%$ of our spectra have this data quality and another 40% have SPEC_QUAL=3, which we consider sufficient for redshift

⁸ <http://www.ucolick.org/~xavier/LowRedux/>

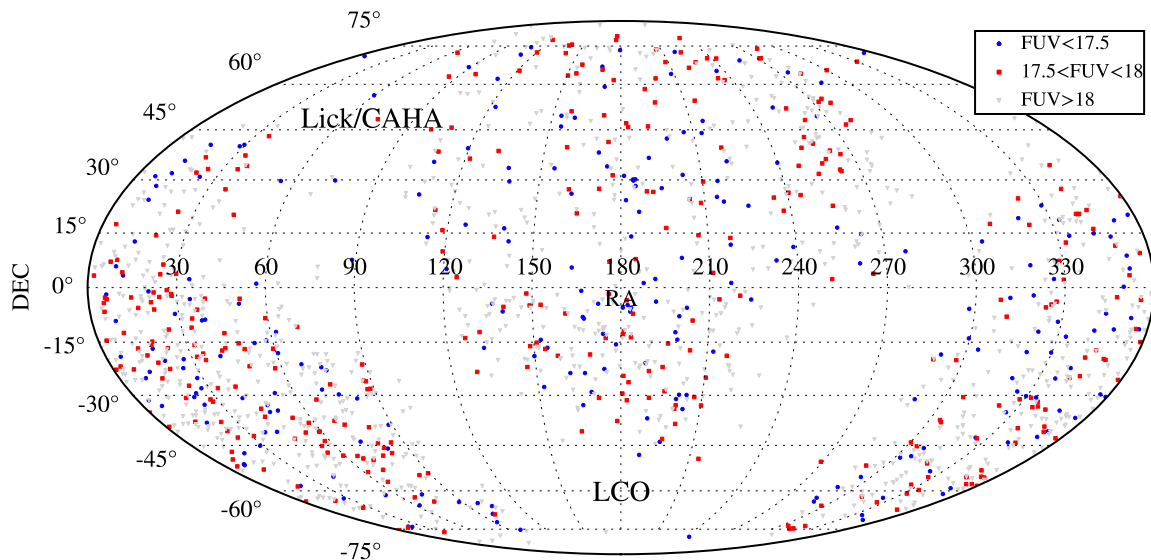


FIG. 2.— An all-sky plot describing the spatial distribution of our primary candidates, coded by FUV flux. We have avoided the Galactic plane and one also notes fewer targets towards the Northern Galactic pole (i.e. within the SDSS footprint).

TABLE 3
UVQS DR1 OBSERVATIONS

Name	Obs.	Inst.	Date	Q ^a
UVQSJ000000.15–200427.7	LCO	BCS	Aug2014	3
UVQSJ000009.65–163441.4	LCO	BCS	Aug2014	3
UVQSJ000503.70–391747.9	LCO	BCS	Aug2014	3
UVQSJ000609.57–261140.5	LCO	BCS	Aug2014	3
UVQSJ000613.28+321534.5	Lick	Kast	Jan2015	2
UVQSJ000717.69+421646.6	Lick	Kast	Jan2015	4
UVQSJ000741.00–635145.8	LCO	BCS	Aug2014	3
UVQSJ000750.78+031733.1	LCO	BCS	Aug2014	4
UVQSJ000755.67+052818.8	LCO	BCS	Aug2014	3
UVQSJ000814.35+121201.3	Lick	Kast	Jan2015	1
UVQSJ000856.77–235317.5	LCO	BCS	Aug2014	4
UVQSJ001015.62–624045.1	LCO	BCS	Aug2014	3
UVQSJ001121.73–200212.1	LCO	BCS	Aug2014	3
UVQSJ001155.60–240438.8	LCO	BCS	Aug2014	4
UVQSJ001444.02–223522.6	LCO	BCS	Aug2014	3
UVQSJ001521.62–385419.1	LCO	BCS	Aug2014	3
UVQSJ001529.53–360535.3	LCO	BCS	Aug2014	3
UVQSJ001637.90–054424.8	Lick	Kast	Jan2015	3
UVQSJ001641.88–312656.6	Magellan	MagE	Jul2014	5
UVQSJ001653.66–530932.6	LCO	BCS	Aug2014	3
UVQSJ001655.68+054822.9	LCO	BCS	Aug2014	3

NOTE. — Table 3 is published in its entirety in the electronic edition, a portion is shown here for guidance regarding its form and content.

^a Spectral quality: 0=Too poor for analysis; 5=Excellent

analysis.

4. REDSHIFT ANALYSIS

To estimate the redshift of each source, we employed modified versions of the SDSS IDLUTILS software designed to measure quasar redshifts in that survey (Schneider et al. 2010). Specifically, we smoothed the quasar eigenspectra of SDSS (file: spEigenQSO-55732.fits) to match the spectral resolution from each of

our instruments and then fit these eigenspectra to each spectrum, minimizing χ^2 . The algorithms provide a best redshift, the model eigenvalues, and a statistical estimate of the redshift uncertainty $\sigma(z)$.

All of the 1D spectra were visually inspected by at least two authors using a custom GUI to assess the spectra quality. In parallel, we assessed the redshift measurement by examining the best-fit on the data. As necessary ($\sim 30\%$ of the cases), we performed our own estimation of the redshift by identifying standard AGN emission features (primarily MgII and H β). We then re-fitted templates to the data using a restricted redshift interval. We assessed the final redshift estimate based on the data quality and the number of spectral features identified and assigned a numerical quality assessment Z_QUAL with a scale of 0 (no estimate possible) to 5 (excellent estimate). Typically, sources with one prominent emission feature with a high-confidence assignment were given Z_QUAL=3. The majority of these are AGN with $z \approx 0.5$ where the Mg II emission line occurs at $\lambda \approx 4000\text{\AA}$ and the expected H β emission features falls redward of our spectral coverage. Many of these spectra show weak Balmer emission (e.g. H γ) and/or continuum features that give high confidence to the reported redshift. Furthermore, associating the detected feature to another emission line (e.g. CIII) is strongly disfavored due to the non-detection of other, expected features. When multiple emission features were detected at a common redshift, the quality of the redshift determinations is given 4 or 5 on our scale. From the total candidate list (Tables 1 and 2), we measured a high-quality redshift (Z_QUAL ≥ 3) for 1121 unique sources.

In the following we assume that every source with recessional velocity $v_r \equiv zc < 500 \text{ km s}^{-1}$ is “Galactic”,

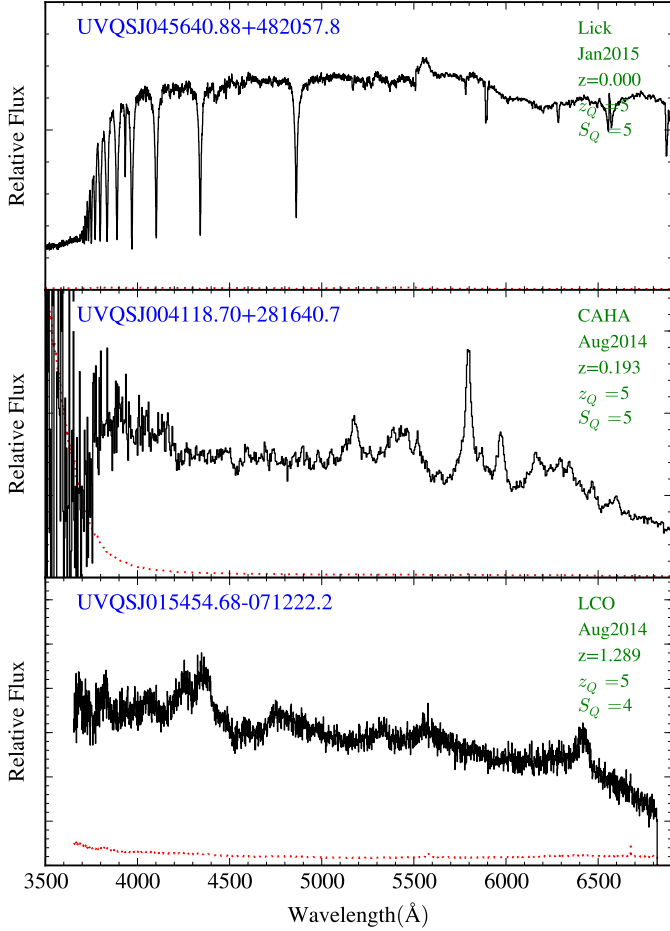


FIG. 3.— Characteristic spectra of the UVQS DR1 data release. From top to bottom, we show examples of a Galactic star, a low- z AGN, and a $z > 1$ quasar.

which we associate to the Galaxy and members of the Local Group. This included sources where the eigenspectra fits were poor yet a low v_r was indisputable (e.g. stars). Many of these were assigned $z = 0$ exactly. The remainder of UVQS sources are assumed to be extragalactic AGN. We caution, however, that we have not assessed the relative line-fluxes of these sources nor assessed the widths of emission-lines to confirm AGN activity. On the other hand, every source has a $W1 - W2$ color in excess of 0.6 mag and is therefore highly probable to contain an AGN⁹. Furthermore, nearly all of these sources exhibit at least one broad emission feature indicative of an AGN.

For the redshift uncertainty of the extragalactic sources, we have adopted the larger of $\sigma(z)$ derived from the eigenspectra analysis and 0.003. The latter value represents a systematic uncertainty from our procedure and also allows for the uncertainties in deriving a systemic redshift from broad, far-UV emission lines (e.g. Richards et al. 2002). We note, however, that many of the sources with $z < 0.5$ exhibit [OIII] emission that may provide a smaller redshift uncertainty.

To assess the quality of our redshift estimates, we have compared our values against the Million Quasar Catalog (MILLIQUAS; v4.5) compiled by Flesch (2015).

⁹ The obvious exception will be chance superpositions of two sources, which we estimate to be a very rare occurrence ($< 1\%$).

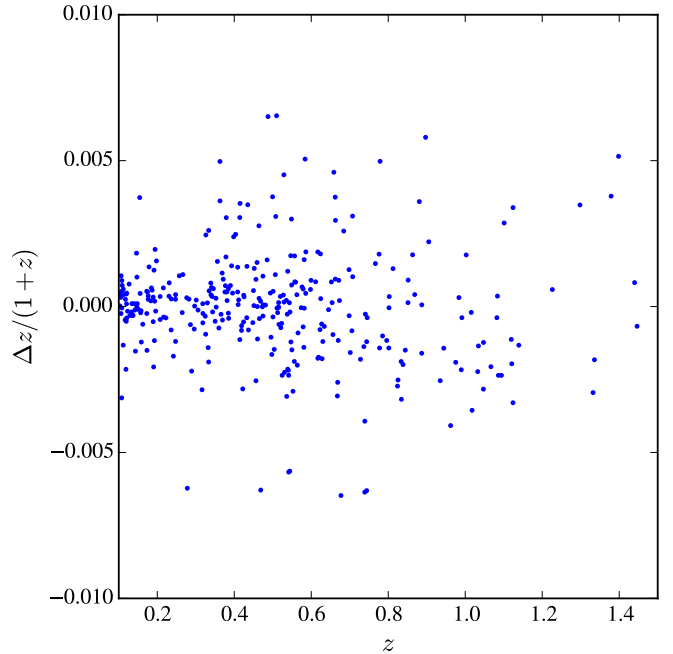


FIG. 4.— Redshift differences between measurements from our UVQS spectroscopy and the values listed in the MILLIQUAS catalog. With the exception of a few outliers (described in the text), there is very good agreement (RMS ≈ 0.002).

We restrict the MILLIQUAS sample to sources with spectroscopic redshifts (TYPE=A or Q) and cross-matched in RA, DEC to a 5 arcsecond radius. In our first assessment, we noted two sources with very large redshift difference: UVQSJ000856.77–235317.5 and UVQSJ231148.97+353541.4. In each of our spectra, there is a single, broad emission feature. For UVQSJ000856.77–235317.5, we had initially identified the feature as CIII] emission yet corresponding C IV emission is not apparent. Therefore, we revised our evaluation to mark this line as MgII emission and revised the redshift accordingly; it is consistent with the previously cataloged value. The other source is a similar case with the line identifications reversed; we have specified the line to be MgII emission. If the line were CIII], as previously assumed, the quasar should have shown MgII emission. Given that there are also weak features at the expected wavelengths of H γ and H β for our preferred redshift, we have maintained our estimate for the source redshift.

Figure 4 summarizes the differences in redshifts $\delta z \equiv \Delta z / (1 + z)$ between our measurements and those previously reported in the literature. Ignoring the anomalous cases described above, we measure an RMS of 0.002 for the 191 sources with $z > 0.1$.

We present a histogram of the sources with well-constrained redshifts ($Z_QUAL \geq 3$) in Figure 5. For the primary candidates (black), there are two distributions at $z \approx 0.1$ and $z \approx 0.5$. The former are low- z AGN while the other set are our desired targets. These exhibit a tail of redshifts to nearly $z = 2$. As expected, the sources drawn from our secondary list of candidates (gray) are primarily at $z < 0.3$; only one has a redshift higher than 0.5. Lastly, the inset to Figure 5 shows the redshift measurements corresponding to $v_r < 1000 \text{ km s}^{-1}$. Again,

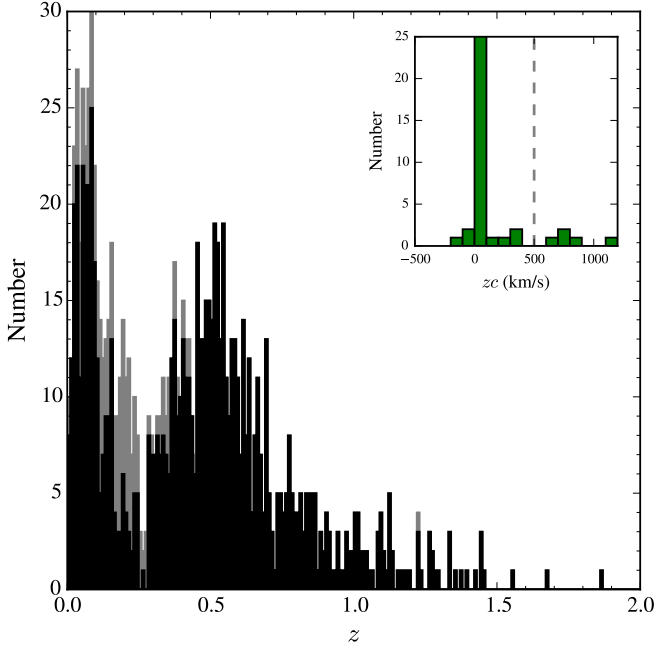


FIG. 5.— Redshift histogram of all sources with $Z_QUAL > 3$ from the UVQ DR1 database. The primary candidates (black) are dominated by sources at $z > 0.4$ with a tail to nearly 2. In contrast, the secondary candidates (grey) are confined to $z < 0.5$ and are primarily at $z < 0.2$. These results further highlight the efficacy of our primary $FUV - NUV$ criterion. The inset shows the recession velocities $v_r \equiv zc$ of sources with $v_r \approx 0 \text{ km s}^{-1}$. We associate all sources with $v_r < 500 \text{ km s}^{-1}$ with the Local Group.

we define those with $v_r < 500 \text{ km s}^{-1}$ to be Galactic, although several could arise from the Local Group or beyond.

5. RESULTS

5.1. The UVQS Sample of New UV-Bright Quasars

The principal goal of the UVQ Survey is to generate a new sample of FUV-bright quasars at $z \sim 1$. This motivated our target color criteria and subsequent observing strategy. With over 1000 sources analyzed, we may reassess the survey design and efficacy. Figure 6 presents the UV and WISE colors of the AGN measured in UVQS DR1, which includes both the primary ($FUV - NUV > 0.6 \text{ mag}$) and secondary ($-0.5 < FUV - NUV < 0.3$) candidates. As the source redshifts increase from $z = 0.1$ to 2, their observed UV and near-IR colors redden. We expect that the UV trend is due primarily to Lyman limit opacity from intervening H I gas, although a flattening of the AGN SED at approximately 1000 \AA could contribute (e.g. Telfer et al. 2002; Lusso et al. 2015). The evolution in $W1 - W2$ color must be intrinsic, i.e. the k -correction for these AGN as this color shifts from the rest-frame near-IR towards the optical (e.g. Assef et al. 2010; Stern et al. 2012). In hindsight, we recognize that one could more efficiently target $z \sim 1$ quasars by adjusting the $W1 - W2$ cut to a larger value (e.g. 1.1 mag).

The efficacy of our survey can be assessed in terms of the fraction of AGN recovered from the total number of sources observed. These results are presented in Figure 7, restricting to the primary candidates. Of 1040 primary candidates observed, we recovered a secure redshift for an

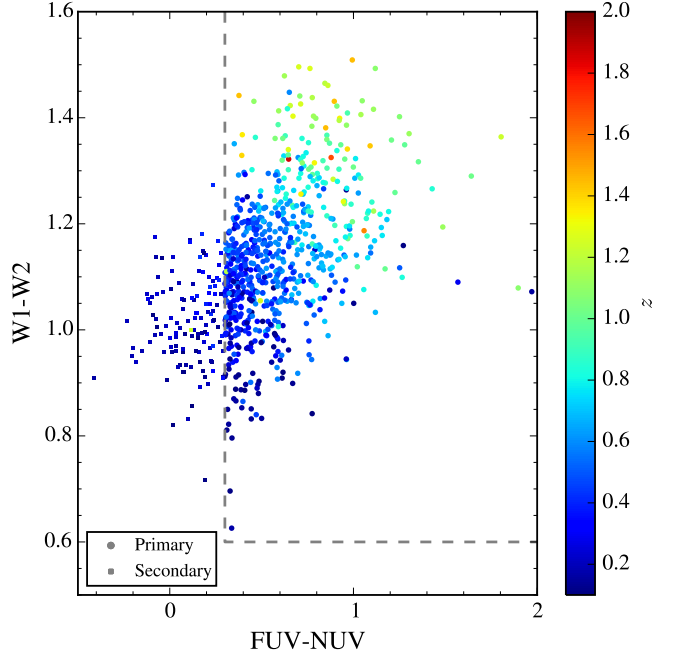


FIG. 6.— Near-IR and UV colors of the UVQS DR1 AGN from the primary (circles) and secondary (square) candidate lists. The AGN show a systematic reddening of both colors with increasing redshift. The near-IR evolution is related to a k -correction whereas we believe the UV evolution is dominated by an increasing average opacity to Lyman limit absorption.

TABLE 4
UVQ DR1 AGN

Name	z	$\sigma(z)^a$	Z_QUAL^b	New? ^c
UVQSJ000000.15-200427.7	0.291	0.003	4	Y
UVQSJ000503.70-391747.9	0.652	0.003	3	N
UVQSJ000609.57-261140.5	0.648	0.003	3	Y
UVQSJ000741.00-635145.8	0.559	0.003	3	N
UVQSJ000750.78+031733.1	1.101	0.003	4	N
UVQSJ000755.67+052818.8	1.098	0.003	4	Y
UVQSJ000856.77-235317.5	0.844	0.003	3	N
UVQSJ001015.62-624045.1	0.850	0.003	3	Y
UVQSJ001121.73-200212.1	1.226	0.003	4	Y
UVQSJ001155.60-240438.8	0.767	0.003	3	N
UVQSJ001521.62-385419.1	0.633	0.003	3	Y
UVQSJ001637.90-054424.8	0.074	0.003	5	Y
UVQSJ001641.88-312656.6	0.360	0.003	5	N
UVQSJ001653.66-530932.6	0.914	0.003	3	Y
UVQSJ001655.68+054822.9	1.060	0.003	3	Y
UVQSJ001705.14-312536.4	0.838	0.003	3	N
UVQSJ001753.32-142310.9	0.945	0.003	3	Y
UVQSJ001859.75+061931.9	0.767	0.003	3	Y
UVQSJ001903.85+423809.0	0.113	0.003	5	Y
UVQSJ002049.31-253829.0	0.645	0.003	3	N
UVQSJ002051.30-190126.8	0.962	0.003	3	N

NOTE. — Table 4 is published in its entirety in the electronic edition, a portion is shown here for guidance regarding its form and content.

^a Redshift uncertainty was derived from a template fit to the spectrum. We report a minimum redshift error of 0.003 from systematic uncertainties.

^b Redshift quality: 0=No constraint, 3=Confident, 5=Excellent

^c Source is greater than 10 arcseconds offset any quasar in the MILLIQUAS catalog (v4.5) with a published spectroscopic redshift.

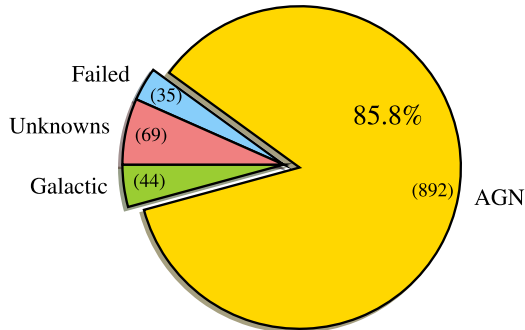


FIG. 7.— Distribution of the source classifications for the primary candidates observed in UVQS DR1. The color-color criteria yielded a very high incidence of AGN. Formally, the reported rate for AGN (86%) is a lower limit as we expect many of the failed and unknown sources are also AGN.

extragalactic AGN for 86% of the objects. The remainder are split rather evenly between Galactic sources, poor spectra, and sources without an evident spectral feature. These are discussed further in the following sections.

Restricting to the $z > 0.6$ quasars from UVQS DR1 that were not listed in the v4.5 of the MILLIQUAS catalog, Figure 8 shows the sky distribution of these new sources. As expected, the majority of the new discoveries occur outside of the SDSS footprint, i.e. towards the Southern Galactic pole. Inspecting several of the sources within the SDSS footprint, we find they have good photometry and expect they were simply not targeted due to fiber collisions.

In Figure 9, we compare the FUV magnitudes and estimated luminosities (without corrections for Galactic extinction) of the new UVQS DR1 AGN. These are compared against previously known sources; specifically, we show a 2D histogram of all sources from the MILLIQUAS catalog laying within 5 arcseconds¹⁰ of an FUV-detected source in the GALEXGR6Plus7 photoobjall catalog. At $z > 0.5$, the UVQS DR1 AGN are among the brightest and most luminous FUV sources known. Follow-up analysis to analyze the Eddington ratio, host galaxies, and galactic environment of these extreme sources may be valuable. Given the high efficiency of our survey, we expect that the community has now identified nearly every FUV-bright quasar on the sky. The only exceptions will be within the areas not surveyed by GALEX and the few lucky sources that shine through the dust of the Galactic plane.

One of the most luminous quasars from our survey, UVQSJ015454.68–071222.2 ($z = 1.289$, $FUV = 17.07$ mag; Figure 3), has an interesting history worth relating. This source was cataloged in 1962 by Haro & Luyten as PHL 1228 (Haro & Luyten 1962). Based on its color and coordinates, those authors identified the source as a candidate faint blue halo star towards the South Galactic pole. Indeed, a number of their candi-

dates have since been confirmed as extragalactic AGN. Clearly, a systematic redshift survey of the complete PHL catalog is warranted.

5.2. Other Sources

Figure 10 shows an all-sky plot of the other UVQS sources: AGN at $z < 0.6$, sources with good spectra but without a precise redshift, and Galactic sources. Not surprisingly, the latter are primarily located near the Galactic plane. In DR1, we observed 66 sources satisfying our color criteria (including 24 with $FUV - NUV < 0.6$ mag) whose spectra yield a recessional velocity $v_r < 500 \text{ km s}^{-1}$. These are listed in Table 5. Spectra for a representative set is shown in Figure 11. These objects include hot stars, white dwarfs, planetary nebulae, and Herbig Ae/Be stars, all of which have high surface temperatures explaining their high UV fluxes. It is more difficult, however, to explain their $W1 - W2$ color. Several of the sources have *WISE* fluxes near their detection limit, i.e. poor photometry may explain their inclusion. Another set have substantial extinction ($E(B - V) > 0.3$ mag). The remainder, however, may be chance super-positions with a low mass star. Finally, we note that from the full set of Galactic sources we identify a small sample with highly unusual spectra (e.g. Margon et al. 2015, submitted).

There are 93 sources with a good quality spectrum ($\text{SPEC_QUAL} \geq 3$) for which we cannot recover a secure redshift. The majority of these have been previously cataloged as blazars (or BL Lac objects). Examining Figure 10 we note these sources are distributed across the sky, consistent with an extragalactic origin. Table 6 lists the sample of these unknowns.

Finally, 48 of the brightest primary candidates ($FUV < 17.5$ mag) went unobserved. Nearly all of these are well resolved in the SDSS or DSS imaging and were dismissed as having $z \ll 1$. Three of the sources – J124735.07-035008.2, J221153.89+184149.9, J221712.27+141420.9 – went unobserved due to errors in book-keeping or insufficient observing time. We will endeavor to provide spectra of these sources in our second data release.

6. CONCLUDING REMARKS

We have performed an all-sky survey for $z \sim 1$, FUV-bright quasars selected from GALEX and WISE photometry. The majority of these candidates lay towards the Southern Galactic Pole, i.e. outside the SDSS footprint. We confirmed 256 AGN at $z > 0.6$, 155 of which had no previously reported spectroscopic redshift. Altogether, the UVQS DR1 includes 217 previously uncataloged AGN with $FUV < 18$ mag which are excellent targets for absorption-line analysis using *HST*/COS. Indeed, a handful of these AGN are already scheduled for Cycle 24 observations. In our second data release of UVQS, we expand the search to NUV-bright AGN at $z \sim 1$.

¹⁰ We caution that a small set of these previously cataloged quasars may have erroneous redshifts (see § 4 for an example) or are a chance coincidence match to the GALEX catalog.

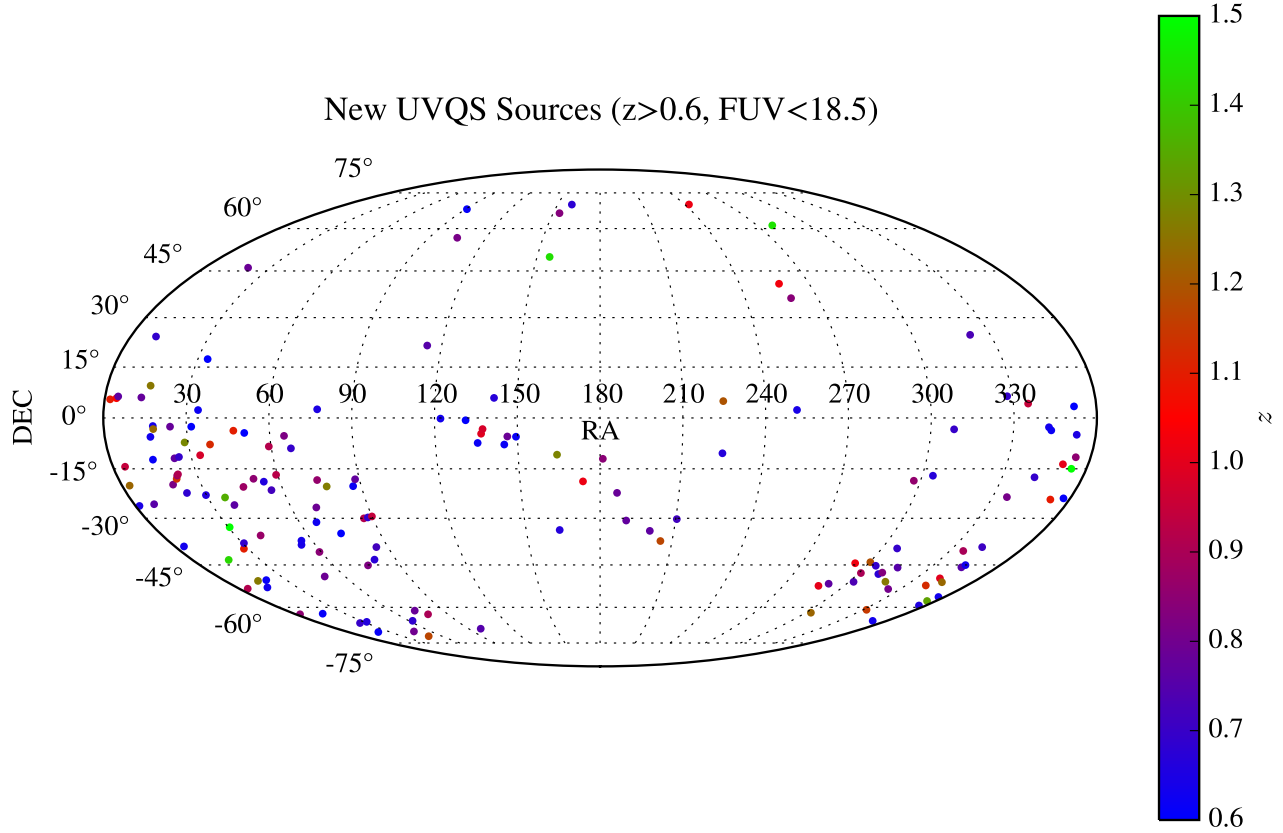


FIG. 8.— All sky distribution of the new FUV-bright AGN at $z > 0.6$, spectroscopically confirmed in our UVQS-DR1 survey. The majority of these lie towards the Southern Galactic Pole.

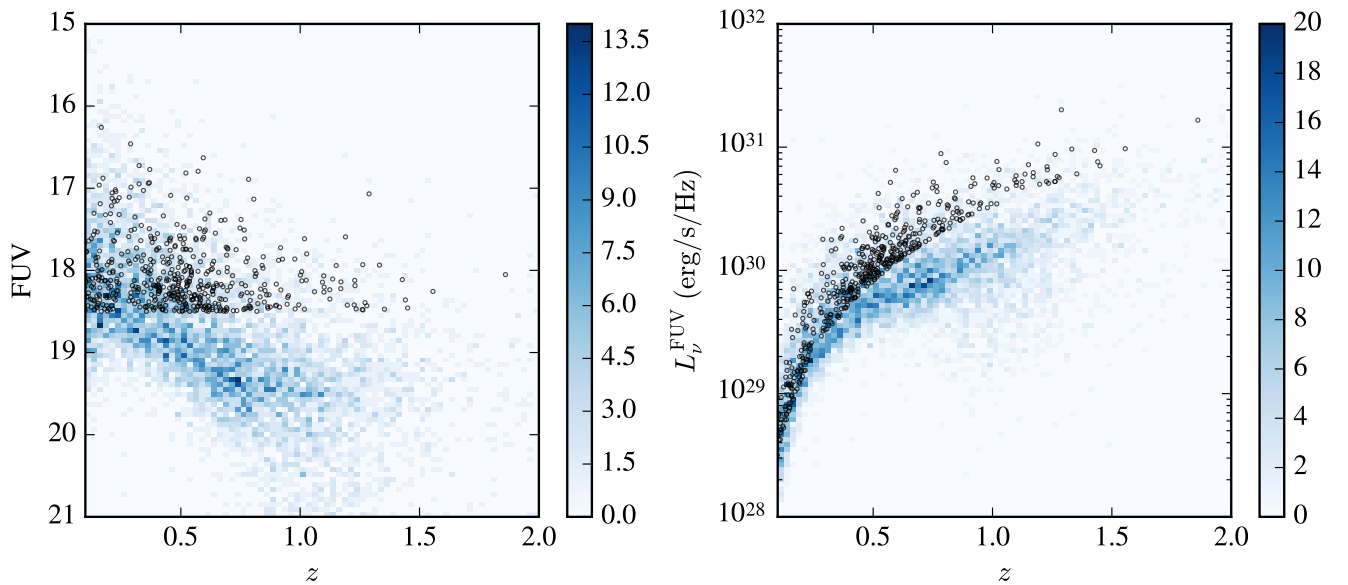


FIG. 9.— (left) FUV GALEX magnitudes for the AGN in the UVQS-DR1 (black dots) compared against the locus of magnitudes from all previously known AGN (blue, 2D histogram). The sources with $FUV < 18$ mag would yield good quality COS spectra in a modest orbit allocation. (right) Specific FUV luminosities with the same symbol and color coding. At $z > 0.5$, the UVQS sources represent the most UV luminous AGN on the sky.

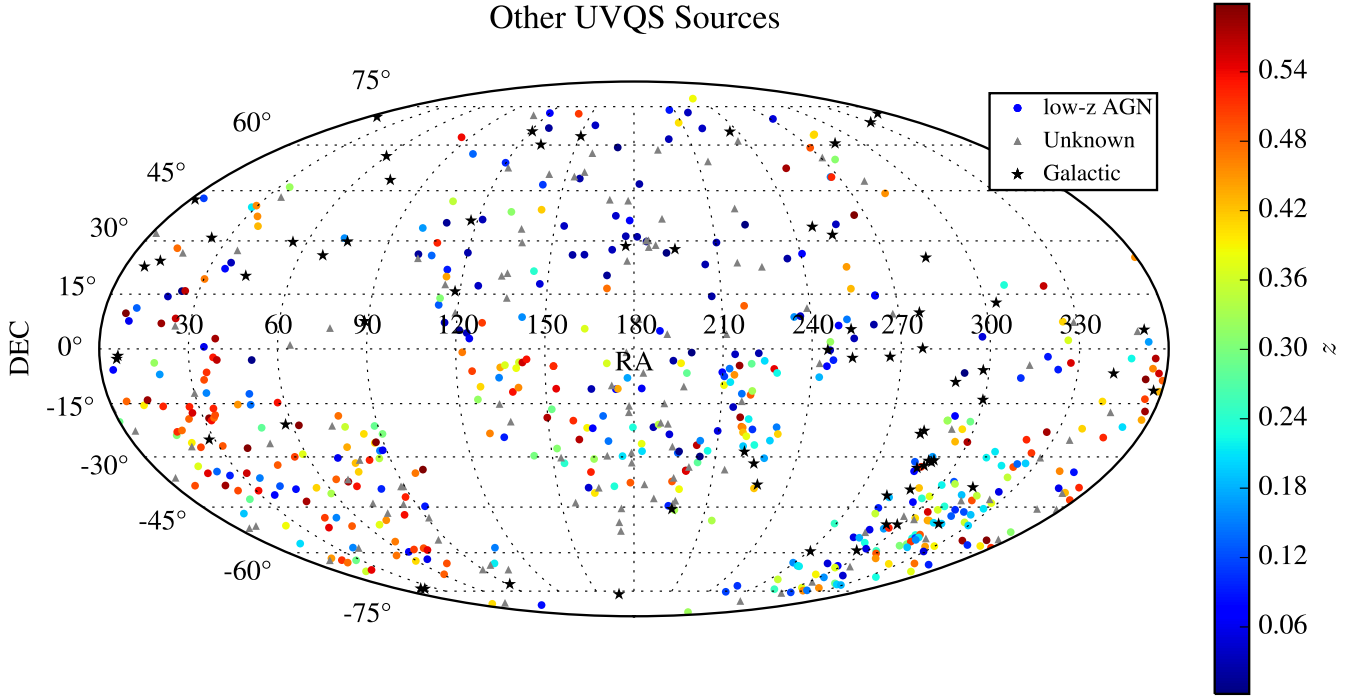


FIG. 10.— All-sky distribution of sources other than $z > 0.6$ AGN drawn from our UVQS-DR1 dataset.

TABLE 5
UVQ DR1 GALACTIC SOURCES

Name	l (deg)	b (deg)	W_1 (mag)	W_2 (mag)	$E(B - V)$ (mag)
UVQSJ000717.69+421646.6	114.2718	-19.8486	12.44	11.51	0.07
UVQSJ002255.11-024418.7	106.0850	-64.6733	13.25	12.12	0.03
UVQSJ002324.11+704009.9	120.5946	7.9250	7.28	6.58	0.95
UVQSJ002452.54-015335.4	107.6594	-63.9745	9.56	8.69	0.03
UVQSJ002715.37+224158.1	115.6634	-39.8307	13.15	11.96	0.04
UVQSJ004433.61+241919.7	120.9291	-38.5229	11.41	10.81	0.05
UVQSJ011219.70-735126.0	300.9427	-43.1902	9.66	8.52	0.04
UVQSJ012138.72-735841.0	300.0898	-42.9831	9.98	9.31	0.05
UVQSJ013450.10+305445.0	133.7961	-31.0421	14.86	13.79	0.05
UVQSJ015159.68-250314.9	207.6540	-76.2551	17.82	16.34	0.01
UVQSJ025637.57+200537.2	158.9238	-33.8856	7.84	7.22	1.24
UVQSJ033900.56+294145.6	161.1830	-20.4629	7.61	6.83	0.22
UVQSJ035056.00-204815.9	214.1511	-48.7234	9.66	9.02	0.07

NOTE. — Table 5 is published in its entirety in the electronic edition, a portion is shown here for guidance regarding its form and content.

TABLE 6
UVQ DR1 UNKNOWN SOURCES

Name	l (deg)	b (deg)	FUV (mag)	NUV (mag)
UVQSJ000009.65-163441.4	71.9317	-74.1194	18.48	17.72
UVQSJ001444.02-223522.6	59.5364	-80.5220	18.39	17.34
UVQSJ001529.53-360535.3	341.1397	-78.2250	18.23	17.70
UVQSJ004038.09-505756.5	307.1282	-66.0744	17.43	16.77
UVQSJ005116.64-624204.3	302.9636	-54.4270	18.31	17.84
UVQSJ010018.69-741815.9	302.1140	-42.8097	17.55	17.12
UVQSJ012031.66-270124.6	213.6632	-83.5246	18.20	17.36
UVQSJ013955.76+061922.4	144.0255	-54.5508	17.64	17.19
UVQSJ022239.60+430207.8	140.1429	-16.7669	17.70	16.88

NOTE. — Table 6 is published in its entirety in the electronic edition, a portion is shown here for guidance regarding its form and content.

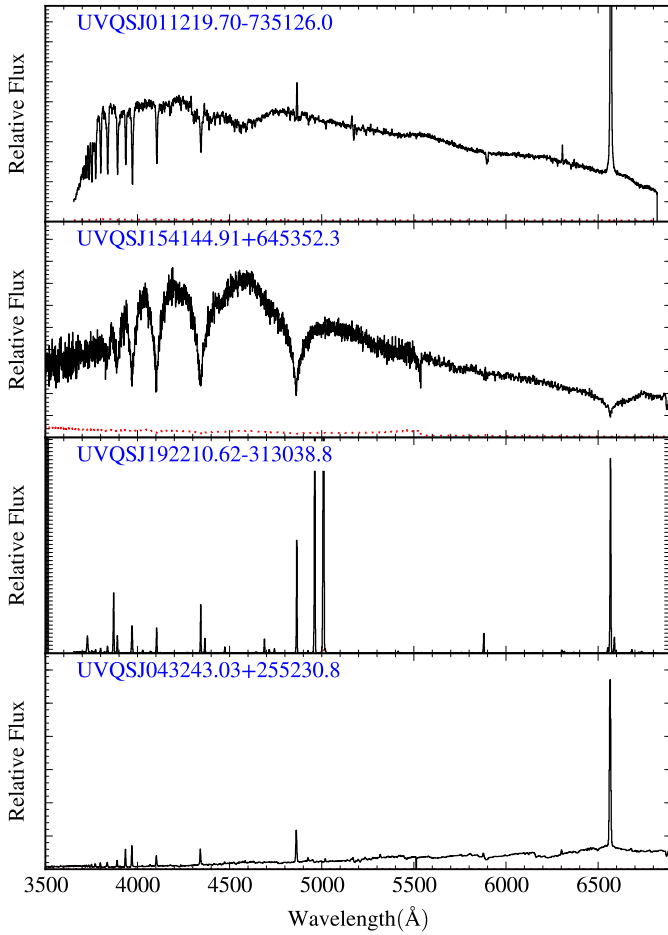


FIG. 11.— UVQS-DR1 spectra for a representative set of Galactic sources unintentionally observed in our survey.

We kindly thank Kate Rubin and Neil Crighton for their twilight observations on several candidates. T. R. M. and J. T. acknowledge support for this project from the STScI Director's Discretionary Research Fund under allocation D0001.82451. J. X. P. and N. T. acknowledge partial support from the National Science Foundation (NSF) grant AST-1412981. JFH acknowledges generous support from the Alexander von Humboldt foundation in the context of the Sofja Kovalevskaja Award. The Humboldt foundation is funded by the German Federal Ministry for Education and Research.

This work is based on data obtained from Lick Observatory, owned and operated by the University of California. We thank the Mount Hamilton staff of Lick Observatory for assistance in acquiring the observations.

Based on observations collected at the Centro Astronómico Hispano Alemán (CAHA) at Calar Alto, operated jointly by the Max-Planck Institut für Astronomie and the Instituto de Astrofísica de Andalucía (CSIC).

Some of the data presented herein were obtained at the W.M. Keck Observatory, which is operated as a sci-

entific partnership among the California Institute of Technology, the University of California, and the National Aeronautics and Space Administration. The Observatory was made possible by the generous financial support of the W.M. Keck Foundation. Some of the Keck data were obtained through the NSF Telescope System Instrumentation Program (TSIP), supported by AURA through the NSF under AURA Cooperative Agreement AST 01-32798 as amended. The authors wish to recognize and acknowledge the very significant cultural role and reverence that the summit of Mauna Kea has always had within the indigenous Hawaiian community. We are most fortunate to have the opportunity to conduct observations from this mountain.

This publication makes use of data products from the Wide-field Infrared Survey Explorer, which is a joint project of the University of California, Los Angeles, and the Jet Propulsion Laboratory/California Institute of Technology, and NEOWISE, which is a project of the Jet Propulsion Laboratory/California Institute of Technology. WISE and NEOWISE are funded by the National Aeronautics and Space Administration.

REFERENCES

- Assef, R. J., et al. 2010, *ApJ*, 713, 970
 Bianchi, L., Conti, A., & Shiao, B. 2014, *Advances in Space Research*, 53, 900
 Flesch, E. W. 2015, *PASA*, 32, 10
 Haro, G., & Luyten, W. J. 1962, *Boletín de los Observatorios Tonantzintla y Tacubaya*, 3, 37
 Lehner, N., et al. 2013, *ApJ*, 770, 138
 Lehner, N., Savage, B. D., Richter, P., Sembach, K. R., Tripp, T. M., & Wakker, B. P. 2007, *ApJ*, 658, 680
 Lusso, E., Worseck, G., Hennawi, J. F., Prochaska, J. X., Vignali, C., Stern, J., & O'Meara, J. M. 2015, *MNRAS*, 449, 4204
 Meiring, J. D., Tripp, T. M., Werk, J. K., Howk, J. C., Jenkins, E. B., Prochaska, J. X., Lehner, N., & Sembach, K. R. 2013, *ApJ*, 767, 49
 Richards, G. T., Vanden Berk, D. E., Reichard, T. A., Hall, P. B., Schneider, D. P., SubbaRao, M., Thakar, A. R., & York, D. G. 2002, *AJ*, 124, 1
 Schlegel, D. J., Finkbeiner, D. P., & Davis, M. 1998, *ApJ*, 500, 525
 Schneider, D. P., et al. 2010, *AJ*, 139, 2360
 Stern, D., et al. 2012, *ApJ*, 753, 30
 Tejos, N., et al. 2014, *MNRAS*, 437, 2017
 —. 2015, *ArXiv e-prints*
 Telfer, R. C., Zheng, W., Kriss, G. A., & Davidsen, A. F. 2002, *ApJ*, 565, 773
 Tripp, T. M., et al. 2011, *Science*, 334, 952
 Tripp, T. M., Sembach, K. R., Bowen, D. V., Savage, B. D., Jenkins, E. B., Lehner, N., & Richter, P. 2008, *ApJS*, 177, 39
 Tumlinson, J., et al. 2013, *ApJ*, 777, 59
 Werk, J. K., Prochaska, J. X., Thom, C., Tumlinson, J., Tripp, T. M., O'Meara, J. M., & Peebles, M. S. 2013, *ApJS*, 204, 17
 Werk, J. K., et al. 2014, *ApJ*, 792, 8